Journal of Colloid and Interface Science 330 (2009) 449–455

Contents lists available at ScienceDirect

Journal of Colloid and Interface Science

www.elsevier.com/locate/jcis

A facile route to design pH-responsive viscoelastic wormlike micelles: Smart use of hydrotropes

Yiyang Lin [a], Xue Han [a], Jianbin Huang [a,*], Honglan Fu [b], Cailan Yu [c]

[a] Beijing National Laboratory for Molecular Sciences (BNLMS), State Key Laboratory for Structural Chemistry of Unstable and Stable Species, College of Chemistry and Molecular Engineering, Peking University, Beijing 100871, People's Republic of China
[b] College of Life Science, Peking University, Beijing 100871, People's Republic of China
[c] CAS Key Laboratory of Photochemistry, Institute of Chemistry, Chinese Academy of Sciences, Beijing 100080, People's Republic of China

ARTICLE INFO

Article history:
Received 4 September 2008
Accepted 23 October 2008
Available online 6 December 2008

Keywords:
pH responsive
Wormlike micelle
Viscoelastic fluid
Hydrotrope

ABSTRACT

A simple and effective route to design pH-responsive viscoelastic wormlike micelles based on commercial compounds is reported. According to this route, pH-sensitive viscoelastic fluids can be easily obtained by introducing a pH-responsive hydrotrope into a surfactant solution. In this paper, the mixed system of cetyltrimethylammonium bromide (CTAB) and potassium phthalic acid (PPA) was studied in detail. This pH-sensitive fluid can be switched between a gellike state and a waterlike state within a narrow pH change. Rheology and DLS results revealed that the pH-sensitive flowing behavior was attributed to the microstructure transition between wormlike micelles and short cylindrical micelles. Combined with fluorescence anisotropy, NMR, and UV–vis, it was demonstrated that the pH response of viscoelastic fluid originated from the different binding abilities of hydrotrope to surfactant as pH varies. Furthermore, different kinds of hydrotropes can be utilized to prepare pH-responsive viscoelastic fluids in the desired pH areas.

1. Introduction

Molecular self-assembly of surfactants based on noncovalent interactions provides a powerful tool for the creation of well-defined structures in the nanometer or micrometer length scale, such as sphere, rod, fiber, disc, and tube [1–5]. Under certain conditions, global micelles may undergo enormous elongation and form very long and highly flexible aggregates, referred to as "wormlike" or "threadlike" micelles. Above a critical concentration c^*, wormlike micelles may entangle into a transient network, which display remarkable viscoelastic properties [6–10]. Viscoelastic wormlike micelles formed by low molecular weight compounds have drawn considerable interest over the past two decades due to their superior properties and wide applications as heat-transfer fluids, drag reduction agents, hard-surface cleaners, fracturing fluids in oil fields, personal care products, and templates for nanomaterial synthesis [11–14]. In recent years, particular interest is focused on the design of viscoelastic fluids that are responsive to external stimuli, such as light [15–17], electric [18], ultrasound [19], pH [20,21], temperature [22–24], and metal ion [25,26]. These stimuli-responsive viscoelastic fluids (called "smart viscoelastic fluids") can find applications in clutches for transmission [27], shock absorbers [28], vibration control [29], and human muscle stimulators [30].

Compared to other external stimuli, pH is a simple and applicable tool for controlling viscoelastic fluids. However, up to now only a few works have been reported concerning pH-responsive viscoelastic fluids based on small organic molecules. Maeda and co-workers have demonstrated that ionization of tetradecyldimethylamine oxide has marked effects on the viscoelastic properties of the micelle solutions. Later, reversible conversion of wormlike micelles to vesicles of oleyldimethylamine oxides with increase of ionization degree was observed by the same group [20,21]. Apart from wormlike micelle solution, hydrogel formed by three-dimensional networks is another kind of viscoelastic fluid that has attracted great attention [31]. Stupp and co-workers have obtained pH-responsive hydrogels constructed by nanofibers with 12 derivatives of peptide-amphiphile molecules [32]. Xu, Li, and co-workers created a reversible sol–gel transition modulated by pH from a multipyridyl-based supergelator [33]. In addition, Hamachi and co-workers reported a pH-responsive supramolecular hydrogel composed of two small amphiphilic molecules [34]. These studies offer the advantage of controllable pH-responsive viscoelastic fluids through a similar strategy, that is, incorporating pH-responsive moieties into amphiphiles covalently through organic synthesis.

However, more effort should be made to overcome the disadvantages of this strategy before these responsive viscoelastic fluids

* Corresponding author. Fax: +86 10 62751708.
E-mail address: jbhuang@pku.edu.cn (J. Huang).

0021-9797/$ – see front matter
doi:10.1016/j.jcis.2008.10.071

can be applied to industrial areas. First, this strategy relies on novel synthetic amphiphiles with pH-responsive functional groups, which require a time-consuming and low-yield organic synthesis. The synthesis process of these novel amphiphiles may greatly restrict further application of these responsive viscoelastic fluids. Second, a given pH-responsive viscoelastic fluid can only be modulated within a suitable pH area, named as pH_{eff}. In principle, the pH_{eff} was mainly determined by the pH-responsive group attached to the amphiphile. For the consideration of industrial applications, it is necessary to prepare different pH-responsive viscoelastic fluids with various pH_{eff}. Consequently, a series of organic syntheses should be conducted to incorporate different pH-responsive functioning groups to amphiphiles. Based on the above consideration, it is necessary to develop a simple and effective route for preparing pH-responsive viscoelastic fluids with various pH_{eff} without complicated organic synthesis.

In this paper, a new strategy for preparing pH-responsive viscoelastic fluids by incorporating pH-responsive moieties to amphiphiles noncovalently is suggested. The mixture of hydrotrope and conventional surfactant was selected since hydrotropes can strongly bind to the amphiphile head group noncovalently through electrostatic attraction and hydrophobic effects, which greatly promotes the elongation of wormlike micelles. In addition, various hydrotropes bearing different pH-responsive groups are commercially available, such as –COOH, $–NH_2$, –ArOH, $–OPO_3H_2$, and $–PO_3H_2$.

From this perspective, a pH-responsive viscoelastic fluid was designed with a conventional surfactant and hydrotrope, i.e., cetyltrimethylammonium bromide (CTAB) and potassium phthalic acid (PPA). This viscoelastic fluid can be switched between highly viscoelastic solution and waterlike solution within a narrow pH change, which was attributed to the transition between wormlike micelles and short cylindrical micelles. Such pH-responsive microstructure transition was rationalized from a perspective of molecular packing with the aid of NMR, UV–vis, and fluorescence anisotropy. Furthermore, a series of pH-responsive viscoelastic fluids with different pH_{eff} was obtained according to this strategy. Finally, the possibility of applying this strategy to design stimuli-responsive self-assembled organization is discussed.

2. Materials and methods

2.1. Materials

Cetyltrimethylammonium bromide and cetylpyridinium bromide were products of A.R. Grade of Beijing Chemical Co. and recrystallized five times from acetone and ethanol before use. 1-Cetyl-3-methylimidazolium bromide was synthesized and purified according to Ref. [48]. Other compounds were of A.R. grade.

2.2. Rheological measurements

The rheological properties of samples were measured with a ThermoHaake RS300 rheometer. Cone and plate geometries were used in each case. The temperature was controlled at 25 ± 0.05 °C. A solvent trap was used to minimize water evaporation. Frequency spectra were conducted in the linear viscoelastic regime of the samples determined from dynamic strain sweep measurements.

2.3. DLS measurements

DLS was performed with a spectrometer (ALV-5000/E/WIN Multiple Tau Digital Correlator) and a Spectra-Physics 2017 200 mW Ar laser (514.5 nm wavelength). The scattering angle was 90°, and the intensity autocorrelation functions were analyzed by using the methods of Contin.

2.4. NMR measurements

^{1}H NMR was carried out in solutions of D_2O with Mercury Plus 300 MHz. The NMR measurement was carried out at 25 °C.

2.5. UV–vis measurements

UV–vis spectra were carried out on a spectrophotometer (Cary 1E, Varian Australia PTY Ltd.) equipped with a thermostated cell holder. The UV–vis measurements were all carried out at 25 °C.

2.6. Fluorescence anisotropy

Steady-state fluorescence anisotropy (r) was measured on a F4500 Hitachi spectrofluorometer equipped with a thermostated cell holder and filter polarizers that used the L-format configuration [35]. 1,6-Diphenyl-1,3,5-hexatriene (DPH) was used as the fluorescence probe. The concentration of DPH was adjusted to 1.0 μmol by adding an appropriate amount of 1.0 mmol ethanol stock solution of the probe. The excitation wavelength was 350 nm and the emission was monitored at 430 nm. The r value was calculated employing the equation

$$r = (I_{VV} - GI_{VH})/(I_{VV} + 2GI_{VH}), \tag{1}$$

where I_{VV} and I_{VH} are the fluorescence intensities polarized parallel and perpendicular to the excitation light, and G is the instrumental correction factor ($G = I_{VV}/I_{VH}$).

3. Results and discussion

3.1. pH-sensitive rheological properties and microstructure transition

Fig. 1a shows the appearance of viscoelastic fluid containing mixtures of 60 mM CTAB and 40 mM PPA. At pH 3.90, the sample is transparent and viscous enough to support its own weight. As pH was adjusted to 5.35, the sample shows a waterlike flowing behavior.

Steady and dynamic rheological measurements were performed to investigate the flowing properties as pH value varies. At pH 3.9, the system shows a shear thinning flowing behavior with a viscosity plateau of 75,000 cP (Fig. 1b). Dynamic rheological measurement (Fig. 1c) indicates a strong viscoelasticity of this solution. The elastic modulus G' and viscous modulus G'' exhibit a good fit to a single-relaxation-time Maxwell model, given by the equations below:

$$G'(\omega) = \frac{G_0(\omega t_R)^2}{1 + (\omega t_R)^2}, \tag{2}$$

$$G''(\omega) = \frac{G_0 \omega t_R}{1 + (\omega t_R)^2}. \tag{3}$$

Here, G_0 is the plateau modulus, and t_R is the relaxation time estimated as $1/\omega_c$, where ω_c is the crossover frequency at which G' and G'' intersect. Also the "Cole–Cole" plot of G'' versus G' (see Fig. S1 in Supplementary material) reveals the semicircle characteristic of a Maxwell fluid, which is expressed as

$$G''^2 + \left(G' - \frac{G_0}{2}\right)^2 = \left(\frac{G_0}{2}\right)^2. \tag{4}$$

The steady shear and dynamic oscillation response strongly suggest the existence of wormlike micelles in the mixture of 60 mM CTAB and 40 mM PPA at pH 3.90.

As pH increases, the viscosity of the sample drops remarkably. When pH reaches 5.35, the sample exhibits a Newtonian flowing behavior with a low shear viscosity of 1.1 cP (Fig. 1b). Dynamic rheological measurement indicates a gradual decrease of elastic

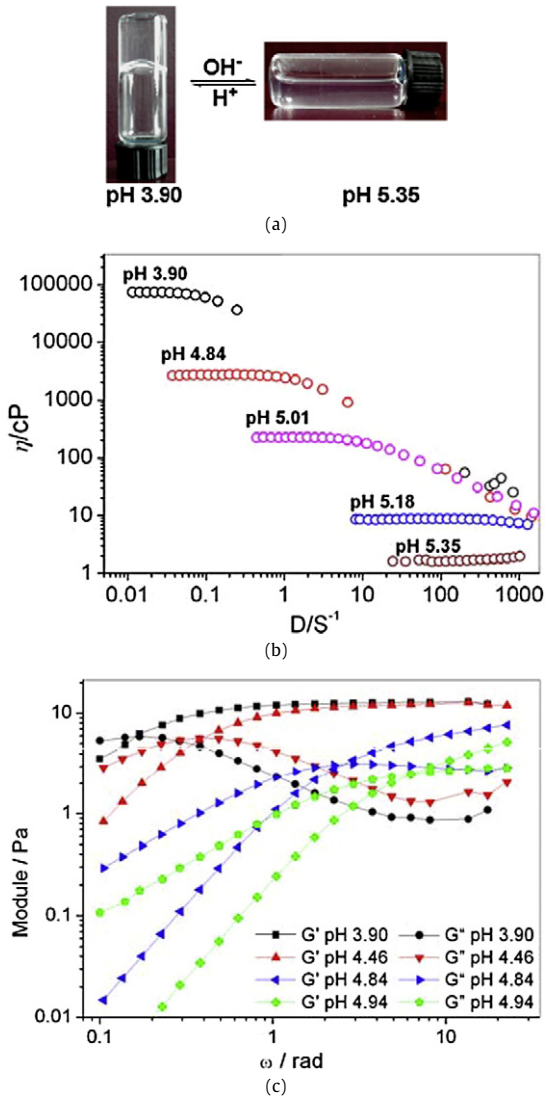

Fig. 1. (a) Macroscopic appearance of the sample with different pH values. (b) Steady shear viscosity plots for 60 mM CTAB and 40 mM PPA with different pH values. (c) Elastic modulus G' and viscous modulus G'' as functions of the angular frequency ω.

moludus G', viscous modulus G'', and a departure from Maxwell model with increasing pH value (Fig. 1c). DLS measurement was performed to reveal the aggregate behavior at pH 5.35. As shown in Fig. 2, a particle with the hydrodynamic radius of 7 nm can be detected, which corresponds to a short cylindrical micelle.

Combined with the results of rheology and DLS, it is suggested that the pH-sensitive flowing behavior is attributed to the transition between wormlike micelle and short cylindrical micelle as pH varies. The strong viscoelasticity or gellike behavior stems from the entanglement of elongated wormlike micelle and the deformation of wormlike micelle causes the decrease of viscosity at high pH.

It is worth noting that the viscosity of the mixture of 60 mM CTAB and 40 mM PPA performs nearly a five order change within narrow pH change (~1.45 pH unit). In addition, the rheological properties of such pH-sensitive fluid can be almost reversibly controlled. As indicated in Fig. 3, the viscosity can be switched between $\sim 10^5$ and $\sim 10^0$ cP by varying the pH for at least three cycles and the sample can be tuned between gellike and waterlike states. The high pH sensitivity and reversible control of rheological properties may greatly facilitate practical applications of such responsive viscoelastic fluid.

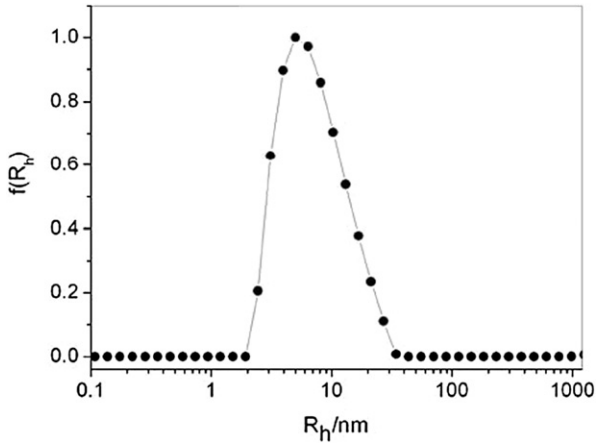

Fig. 2. Hydrodynamic radius (R_h) distributions of the CTAB and PPA system at pH 5.35.

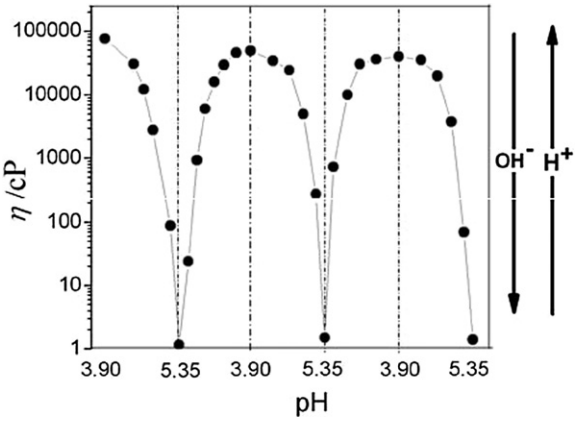

Fig. 3. Viscosity of 60 mM CTAB and 40 mM PPA during the repeated cycles of pH variation.

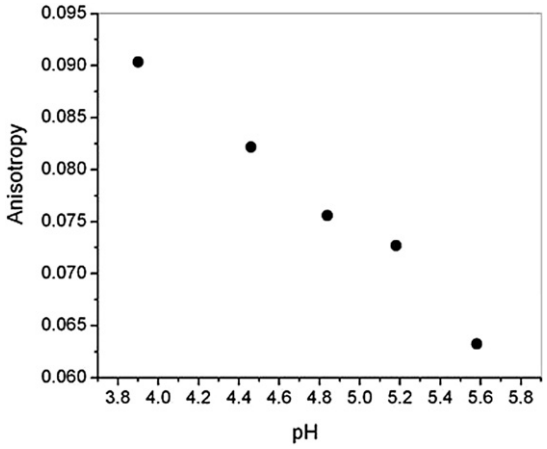

Fig. 4. Fluorescence anisotropy r of DPH in 60 mM CTAB and 40 mM PPA with variation of pH.

3.2. Fluorescence anisotropy study

Depolarization degree of fluorescence emission is an indication of the rotational diffusion of an excited fluorophore and is widely exploited to probe the microenvironment in the organized microstructure. Here, the polarization degree of the DPH fluorescence was expressed by the fluorescence anisotropy r. Fig. 4 shows the DPH fluorescence anisotropy in the system of 60 mM CTAB and 40 mM PPA at different pH values. It can be noted that the

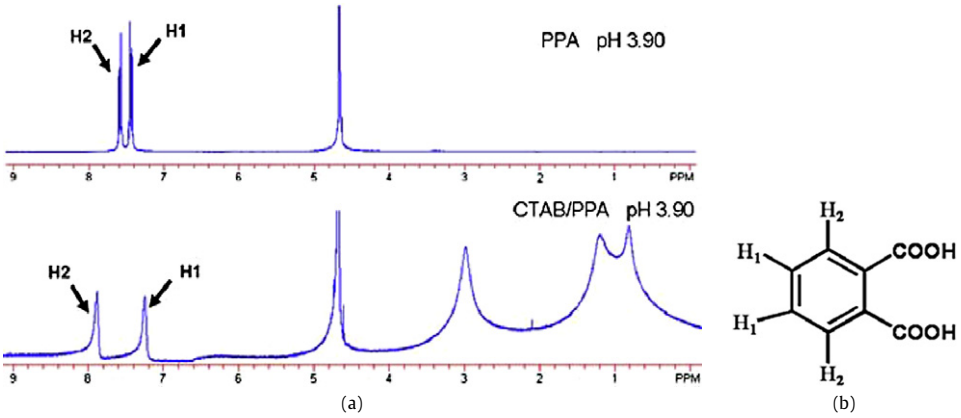

Fig. 5. (a) Proton resonances for PPA and CTAB/PPA solution at pH 3.90. (b) The chemical structure of PPA molecule.

fluorescence anisotropy of DPH monotonously lowers as pH value increases, indicating a decrease of fluorescence polarization degree at high pH. Thus it is believed that the rotation of DPH was facilitated as the pH rises. Considering the fact that DPH was solubilized into the hydrocarbon chain, it can be confirmed that the hydrocarbon chain in the micelle tends to a looser packing at high pH. According to the molecular packing parameter, the looser packing may result in small aggregates, e.g., global micelles or short cylindrical micelles.

3.3. ^1H NMR measurement

NMR is a powerful tool for studying the association between hydrotrope and amphiphile [36–38]. Herein, ^{1}H NMR measurement was carried out at different pH values in order to gain a deeper insight into the molecular interaction between PPA and CTAB.

Fig. 5a shows the proton resonances of 40 mM PPA in the absence and presence of CTAB at pH 3.90. Two proton resonance peaks of PPA aromatic ring were assigned as indicated in Fig. 5b. It can be noted from Fig. 5a that the protons on aromatic ring show an apparent shift with addition of CTAB: the proton H1 shifted to upfield while the proton H2 shifted to downfield. The NMR signal shift can be rationalized as follows: (1) in the absence of CTAB, H1 was exposed to the bulk water and experienced a polar environment; with addition of CTAB, PPA strongly binds to the CTAB head group with the aromatic ring penetrating into hydrocarbon chains through hydrophobic effects and electrostatic attraction. In other words, proton H1 undergoes from a polar environment to an apolar environment and as a result the NMR signal shifted to upfield [36–38]. (2) In contrast, H2 undergoes a downfield shift with addition of CTAB and it was also attributed to the binding of PPA to CTAB and the interaction between the $^+N(CH_3)_3$ head group and the proton H2 [36,37].

In order to better discuss the interaction between PPA and CTAB, a new parameter $\Delta\delta$ was defined as

$$\Delta\delta = \delta' - \delta,$$

where δ and δ' are the chemical shift of the proton on the PPA aromatic rings in the absence and presence of CTAB, respectively. As discussed above, the signal shift change $\Delta\delta$ was caused by the interaction between PPA and CTAB: strong binding of PPA to CTAB results in a large signal shift change. In turn, the value of $\Delta\delta$ can qualitatively scale the binding ability of PPA to CTAB.

A NMR experiment in the absence and presence of CTAB was also carried out at pH 4.46, 4.84, 5.18, and 5.45 (see Fig. S2 in Supplementary material). A plot of $\Delta\delta$(H1) and $\Delta\delta$(H2) as a function of pH value is shown in Fig. 6. It can be noted that the signal shift change $\Delta\delta$ for both H1 and H2 was gradually reduced as the pH rises. Considering the fact that $\Delta\delta$ was caused by the binding of hydrotrope to CTAB, it can be confirmed that the binding of hydrotrope to CTAB was weakened as the pH increases.

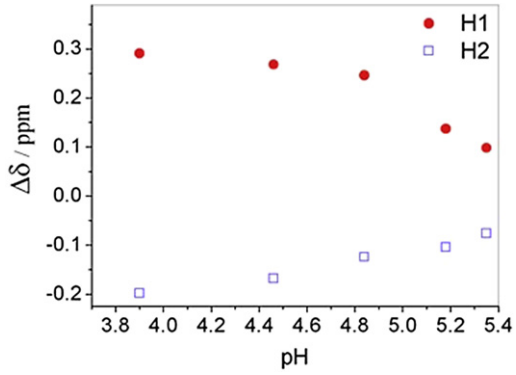

Fig. 6. Variation of proton chemical shift change $\Delta\delta$ on the aromatic ring at different pH values.

3.4. UV–vis spectra

In order to further investigate the interaction between CTAB and aromatic rings as the pH varies, UV–vis measurement was performed. As shown in Fig. 7a, the PPA solution shows a maximal absorbance λ_{max} in 283 nm in the absence of CTAB. With addition of CTAB, the λ_{max} shifted to 286 nm and a broad shoulder can be easily noted. According to previous reports [39], the red shift of absorbance was attributed to the strong cation–pi interaction between the aromatic ring of PPA and the CTAB head group. As pH increases, PPA transforms into DPPA (dipotassium phthalic acid) and no red shift can be observed with the addition of CTAB (Fig. 7b). Therefore it can be confirmed again that the binding ability of hydrotrope to the CTAB head group was weakened with increasing pH, which is in accord with NMR result.

3.5. Interpretation of pH-responsive aggregate transition and rheological response

From the result of rheology and DLS, the peculiar pH-sensitive rheological property was ascribed to the aggregate transition between wormlike micelle and short cylindrical micelle. In this section, we try to explore the origin of pH-responsive aggregate behavior combined with the results of NMR, UV–vis, and fluorescence anisotropy.

It is well known that phthalic acid has two carboxyl acid groups which can be ionized depending on the solution pH. The pK_{a1} and pK_{a2} of phthalic acid were 2.90 and 5.40, respectively. In this study, we mainly focus on the solution condition with pH ranging from

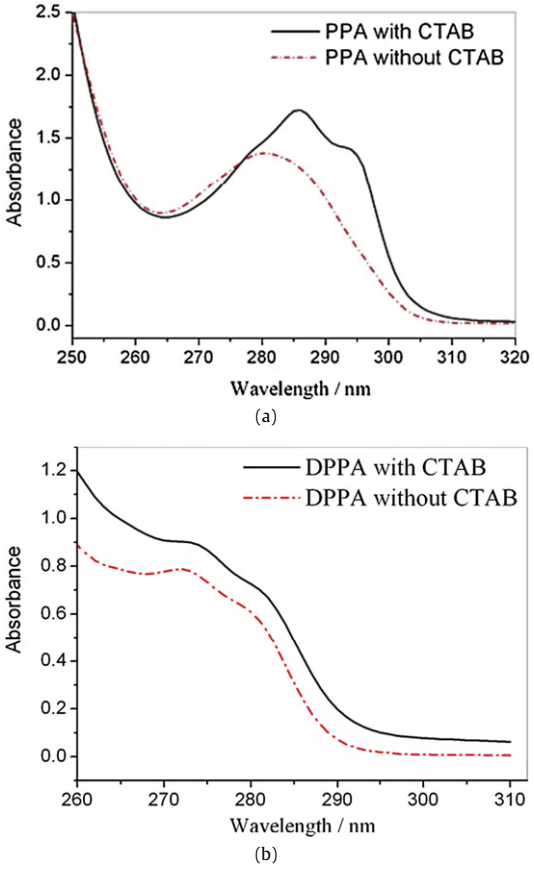

Fig. 7. (a) UV–vis spectra of 1 mM PPA in the presence and absence of CTAB. (b) UV–vis spectra of 1 mM DPPA in the presence and absence of CTAB.

3.90 to 5.35. As shown in Fig. S3, potassium phthalic acid is the dominant structure (~88%) in solution at pH 3.90. Owing to special molecular structure with an aromatic group and one ionized carboxylic acid moiety, potassium phthalic acid can be regarded as a hydrotrope. Hydrotropes are a class of amphiphilic compounds that can show an ability to increase the solubility of sparingly soluble organic molecules in water and reduce the surface tension of water. The common molecular characteristic of a hydrotrope is an aromatic ring and an ionic moiety. Many studies have illustrated the binding ability of hydrotropes to ionic surfactant head groups through hydrophobic effects and electrostatic attraction. Herein, the surface tension of PPA in aqueous solution was measured (Fig. S4). It can be noted that PPA has the ability to reduce the surface tension of water at certain concentrations and thus can be regarded as a hydrotrope. In this paper, we have demonstrated that PPA can strongly bind to the CTAB head group noncovalently with the results of NMR and UV–vis. Owing to the interaction of PPA and CTAB, the electrostatic repulsion between CTAB head groups was screened and the hydrocarbon chain packing becomes tighter as indicated by fluorescence anisotropy of DPH. According to the molecular packing parameter [40], large aggregates were preferred when a tight molecule packing was achieved.

As the pH increases with the addition of KOH, PPA molecule (potassium phthalic acid) transformed into DPPA. DPPA exhibits different physicochemical properties due to the special molecular structure of two ionized carboxylic acid moieties. First, the solubility of DPPA (~1.5 M) is larger than that of PPA (~0.7 M), indicating more hydrophilicity of DPPA. Second, the surface activity of DPPA is weaker than that of PPA (see Fig. S4). Thus it can be suggested that DPPA is more hydrophilic than PPA due to two ionized carboxylic acid moieties and cannot effectively bind to the CTAB head group. As a result, the electrostatic repulsion between CTAB head groups cannot be shielded and a loose packing between hydrocarbon chains was adapted. Consequently short cylindrical micelles formed at high pH. So we can conclude that the pH-responsive aggregate behavior originated from the pH-dependent hydrophilicity of hydrotrope PPA and the binding ability to CTAB head group.

In summary, pH can be utilized to change the molecular structure and hydrophilicity of hydrotropes which may result in the variation of molecular interaction between surfactant and hydrotrope. As a result, pH-responsive microscopic assembly and the corresponding macroscopic rheological properties can be obtained by varying pH. A representative scheme is illustrated in Fig. 8.

3.6. Design pH-responsive viscoelastic fluids with different pH_{eff}

According to the above analysis, a hydrotrope-bearing pH-responsive group can be utilized for constructing pH-responsive viscoelastic wormlike micelles. A variation of hydrotropes and amphiphiles has been applied to design pH-responsive viscoelastic fluids as listed in Fig. 9.

An important parameter of the pH-responsive viscoelastic fluids is the pH area in which the rheological properties can be effectively modulated, called pH_{eff}. As discussed in Section 3.6, the pH_{eff} is mainly determined by the pK_a of hydrotrope. Thus it is anticipated that pH_{eff} can be tuned by introducing different hydrotropes with different pK_a to the surfactant solution. Based on this viewpoint, three hydrotropes with different pK_a, i.e., potassium phthalic acid, 2-naphthyl phosphate monosodium, and 3-hydroxybenzoic acid, were added to CTAB solution, respectively. Fig. 10 shows the pH dependence of solution viscosity in the mixture of CTAB and three hydrotropes. The pK_a and the corresponding molecular

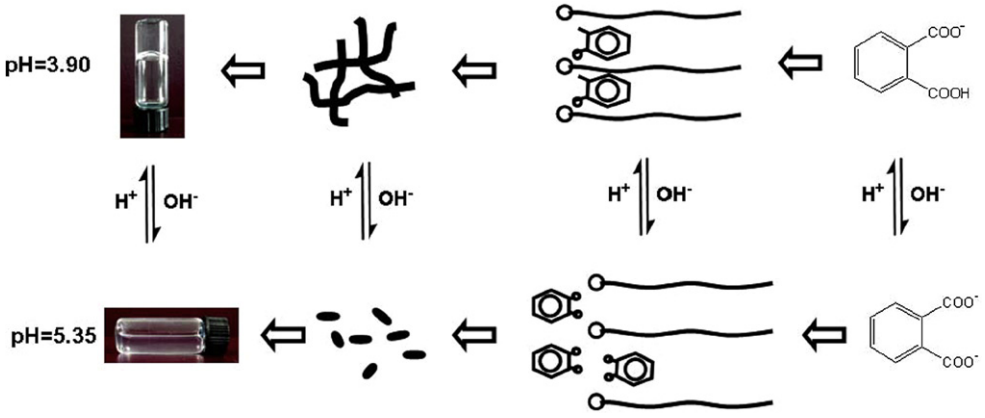

Fig. 8. Schematic representation of the self-assembled organization from wormlike micelle to short cylindrical micelle with pH variation.

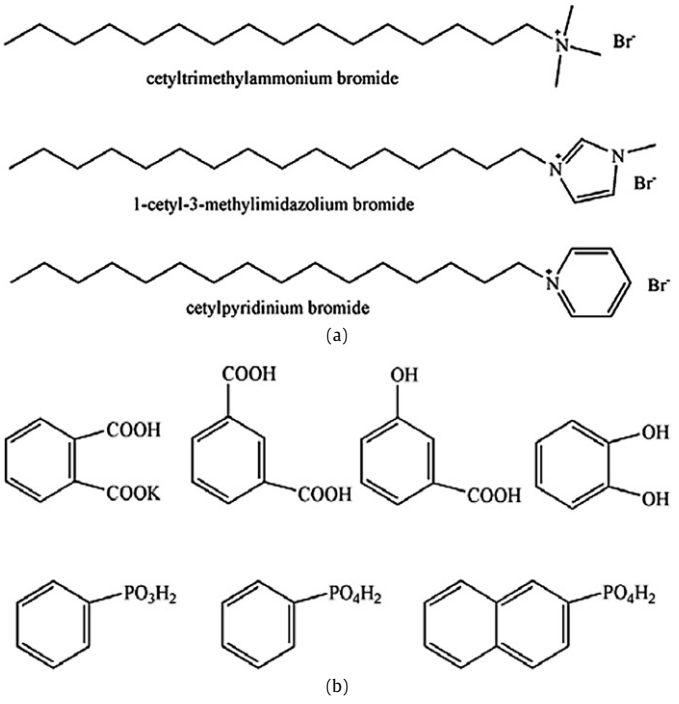

Fig. 9. Surfactants (a) and hydrotropes (b) that have been utilized for preparing pH-responsive fluids.

structure change in the pH area are also indicated in Fig. 10. As expected, pH_{eff} can be shifted to designed areas in the CTAB solution with addition of different hydrotropes. Thus, more pH-responsive viscoelastic wormlike micelles can be generated by utilizing different hydrotropes.

4. Summary

In conclusion, a novel approach to design pH-responsive viscoelastic fluid was reported. Such pH-responsive viscoelastic fluids possess three main advantages: (1) they can be easily obtained with cheap commercial compounds; (2) the rheological behavior can be almost reversibly switched by pH; (3) the pH_{eff} can be tuned when using different hydrotropes. The pH-responsive viscoelastic response was ascribed to the microstructure transition between wormlike micelle and short cylindrical micelle. Further study with NMR, UV–vis, and fluorescence anisotropy revealed that the pH-responsive aggregate transition originated from the variation of molecular interaction of hydrotrope and amphiphile at different pH.

It is well documented that diverse complex organized structures, including micelle, vesicle, tube, and disk can be fabricated in the system of surfactant and hydrotrope [41–47]. When hydrotrope was endowed with stimuli responsibility, the resultant organized structures (e.g., vesicle, tube, or micelles) formed by the mixture of hydrotrope and surfactant can be expected to be responsive to light, electric, temperature, or ultrasound. This may be a simple and promising strategy for fabricating stimuli-responsive organized structures based on common commercial compounds. Further work is still going on in our lab. We hope our work can shed light on the academic research and applications in the amphiphile organized self-assembly world.

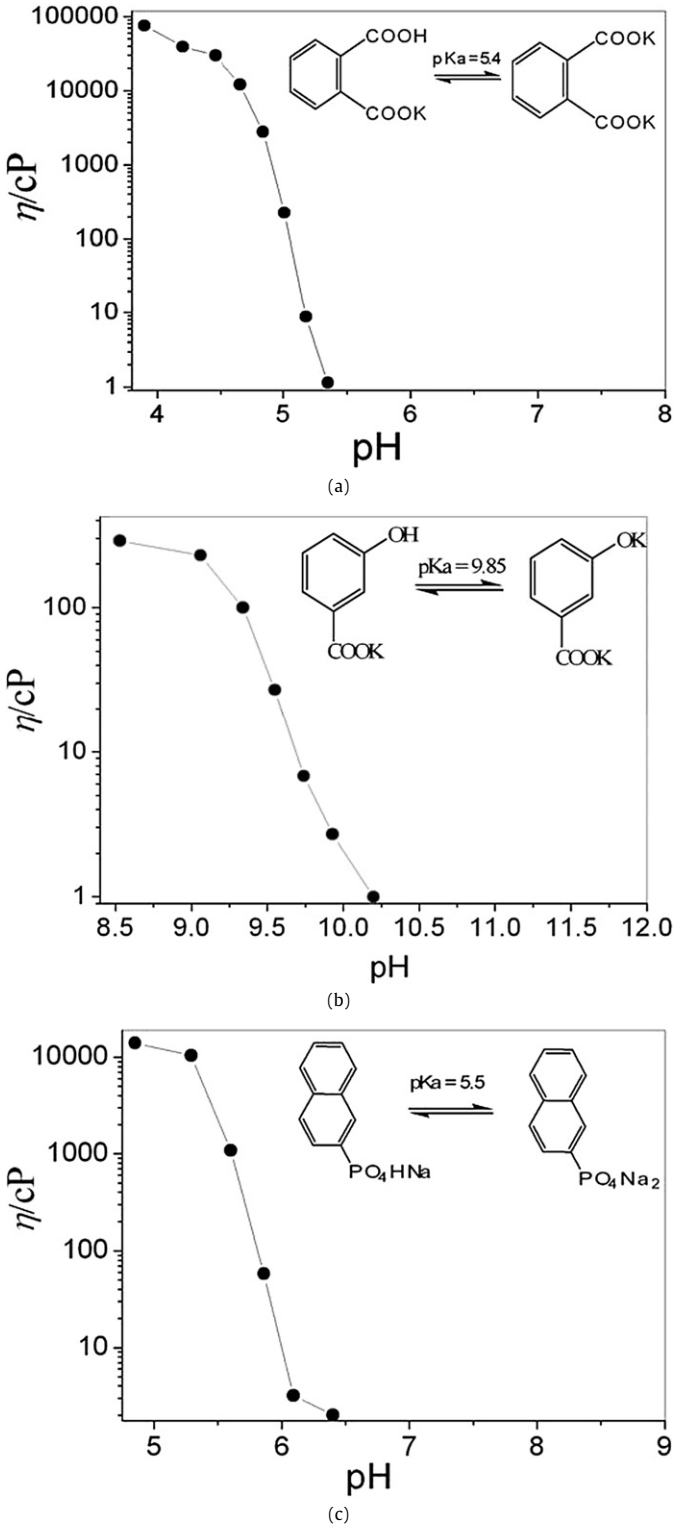

Fig. 10. The pH dependence of viscosity in the systems of 60 mM CTAB and 40 mM different hydrotropes: (a) potassium phthalic acid; (b) 3-hydroxybenzoic acid; (c) 2-naphthyl phosphate monosodium.

Acknowledgments

This work was supported by National Natural Science Foundation of China and National Basic Research Program of China (Grant 2007CB936201).

Supplementary material

Supplementary data for this article may be found in the online version at DOI: 10.1016/j.jcis.2008.10.071. The data include Cole–Cole plot of the viscoelastic fluid, NMR spectrum of CTAB/PPA, and species distribution of PPA molecules in aqueous solution at different pH values.

References

[1] E.W. Kaler, A.K. Murthy, B. Rodriguez, J.A.N. Zasadzinski, Science 245 (1989) 1371.
[2] J.C. Hao, H. Hoffmann, Adv. Colloid Interface Sci. 9 (2004) 279.
[3] Th. Zemb, M. Dubois, B. Demé, Th. Gulik-Krzywicki, Science 283 (1999) 816.
[4] S. Svenson, Curr. Opin. Colloid Interface Sci. 9 (2004) 201.
[5] J.-H. Fuhrhop, W. Helfrich, Chem. Rev. 93 (1993) 1565.
[6] M.E. Cates, S.J. Candau, J. Phys. Condens. Matter 2 (1990) 6869.
[7] D.P. Acharya, H. Kunieda, Adv. Colloid Interface Sci. 123 (2006) 401.
[8] Y.I. Gonzalez, E.W. Kaler, Curr. Opin. Colloid Interface Sci. 10 (2005) 256.
[9] L.M. Walker, Curr. Opin. Colloid Interface Sci. 6 (2001) 451.
[10] S.J. Candau, E. Hirsch, R. Zana, J. Colloid Interface Sci. 105 (1985) 521.
[11] J.L. Zakin, H.W. Bewersdorff, Rev. Chem. Eng. 14 (1998) 2553.
[12] G.C. Maitland, Curr. Opin. Colloid Interface Sci. 5 (2000) 301.
[13] J. Yang, Curr. Opin. Colloid Interface Sci. 7 (2002) 276.
[14] Y.J. Song, R.M. Garcia, R.M. Dorin, H.R. Wang, Y. Qiu, E.N. Coker, W.A. Steen, J.E. Miller, J.A. Shelnutt, Nano Lett. 7 (2007) 3650.
[15] H. Sakai, Y. Orihara, H. Kodashima, A. Matsumura, T. Ohkubo, K. Tsuchiya, M. Abe, J. Am. Chem. Soc. 127 (2005) 13454.
[16] J. Eastoe, A. Vesperinas, Soft Matter 1 (2005) 338.
[17] A.M. Ketner, R. Kumar, T.S. Davies, P.W. Elder, S.R. Raghavan, J. Am. Chem. Soc. 129 (2007) 1553.
[18] K. Tsuchiya, Y. Orihara, Y. Kondo, N. Yoshino, T. Ohkubo, H. Sakai, M. Abe, J. Am. Chem. Soc. 126 (2004) 12282.
[19] J.M.J. Paulusse, R.P. Sijbesma, Angew. Chem. 116 (2004) 4560;
J.M.J. Paulusse, R.P. Sijbesma, Angew. Chem. Int. Ed. 43 (2004) 4460.
[20] H. Maeda, A. Yamamoto, H. Kawasaki, M. Souda, K.S. Hossain, N. Nemoto, M. Almgren, J. Phys. Chem. B 105 (2001) 5411.
[21] H. Kawasaki, M. Souda, S. Tanaka, N. Nemoto, G. Karlsson, M. Almgren, H. Maeda, J. Phys. Chem. B 106 (2002) 1524.
[22] P.A. Hassan, B.S. Valaulikar, C. Manohar, F. Kern, L. Bourdieu, S.J. Candau, Langmuir 12 (1996) 4350.
[23] R.T. Buwalda, M.C.A. Stuart, J.B.F.N. Engberts, Langmuir 16 (2000) 6780.
[24] T.S. Davies, A.M. Ketner, S.R. Raghavan, J. Am. Chem. Soc. 128 (2006) 6669.
[25] J.H. Mu, G.Z. Li, X.L. Jia, H.X. Wang, G.Y. Zhang, J. Phys. Chem. B 106 (2002) 11685.
[26] J.C. Hao, J.Z. Wang, W.M. Liu, R. Abdel-Rahem, H. Hoffmann, J. Phys. Chem. B 108 (2004) 1168.
[27] D.L. Hartsock, R.F. Novak, G.J. Chaundy, J. Rheol. 25 (1991) 1305.
[28] H. Block, J.P. Kelley, J. Phys. D Appl. Phys. 21 (1988) 1661.
[29] R. Stanway, J.L. Sproston, A.K. El-Wahed, Smart Mater. Struct. 5 (1996) 464.
[30] K. Bohon, S. Krause, J. Polym. Sci. Part B Polym. Phys. 36 (1998) 1091.
[31] L.A. Estroff, A.D. Hamilton, Chem. Rev. 104 (2004) 1201.
[32] J.D. Hartgerink, E. Beniash, S.I. Stupp, Proc. Natl. Acad. Sci. USA 99 (2001) 5133.
[33] N.E. Shi, H. Dong, G. Yin, Z. Xu, S.H. Li, Adv. Funct. Mater. 17 (2007) 1837.
[34] S.L. Zhou, S. Matsumoto, H.D. Tian, H. Yamane, A. Ojida, S. Kiyonaka, I. Hamachi, Chem. Eur. J. 11 (2005) 1130.
[35] J.R. Lakowica, Principles of Fluorescence Spectroscopy, Plenum, New York, 1983.
[36] T. Shikata, H. Hirata, T. Kotaka, Langmuir 4 (1988) 354.
[37] S.J. Bachofer, U. Simonis, T.A. Nowicki, J. Phys. Chem. 95 (1991) 480.
[38] M. Vermather, P. Stiles, S.J. Bachofer, U. Simonis, Langmuir 18 (2002) 1030.
[39] R.J. Hua, S.J. Aoki, Chem. Soc. Faraday Trans. 93 (1997) 3945.
[40] J.N. Israelachvili, D.J. Mitchell, B.W. Ninhem, J. Chem. Soc. Faraday Trans. 2 (1976) 72, 1525.
[41] R. Abdel-Rahem, H. Hoffmann, J. Colloid Interface Sci. 312 (2007) 146.
[42] P.A. Hassan, S.R. Raghavan, E.W. Kaler, Langmuir 18 (2002) 2543.
[43] H. Hoffmann, H. Rehage, J. Phys. Chem. 92 (1988) 4712.
[44] R. Abdel-Rahem, Adv. Colloid Interface Sci. 141 (2008) 24.
[45] M. Singh, C. Ford, V. Agarwal, G. Fritz, A. Bose, V.T. John, G.L. McPherson, Langmuir 20 (2004) 9931.
[46] L.M. Zhai, B. Herzog, M. Drechsler, H. Hoffmann, J. Phys. Chem. B 110 (2006) 17699.
[47] B. Dong, J. Zhang, L. Zheng, S. Wang, X. Li, T. Inoue, J. Colloid Interface Sci. 319 (2008) 338.
[48] R. Vanyur, L. Biczok, Z. Miskolczy, Colloids Surf. A 299 (2007) 256.